JOURNAL OF SOLID STATE CHEMISTRY 65, 383–391 (1986)

Microdomains in the $CaFe_xMn_{1-x}O_{3-y}$ Ferrites

II. Oxidation and Reduction of the $x = 0.4$ Composition

M. A. ALARIO-FRANCO, J. M. GONZÁLEZ-CALBET, AND M. VALLET-REGÍ

Departamento de Química Inorgánica, Facultad de Químicas, Universidad Complutense, 28040 Madrid, Spain

Received December 31, 1985; in revised form April 17, 1986

It is shown that in the processes of oxidation, reduction, and annealing of samples of the title, three-dimensional microdomains (3D-μD) play a predominant role. These microdomains are intergrown in the three dimensions and allow compositional variations in a very subtile manner. The existence of microdomains seems to be associated with the presence of tetravalent cations and with the fact that all the structures observed are superstructures of the perovskite cell. © 1986 Academic Press, Inc.

Introduction

There are many ways in which solids are built and, indeed, there are many more ways in which the structures of crystalline solids can be described. Although in crystallographic terms there is always a "smallest possible cell," this one can sometimes be described in terms of simpler unit cells of simpler structures which are combined in a number of ways to give the former.

It is also clear that the ways in which these simpler structures can combine are also quite varied (*1*) and range from interpenetration, the simplest example of which is the NaCl structure, to intergrowth (*2*), in which two or more slabs of different structures recur periodically.

Although this periodicity is usually parallel to one particular direction, so that the slabs are infinite in two dimensions and of limited extent in the third (*3, 4*), there are some cases in which the intergrowth recurs (cyclically) in two dimensions (*5, 6*).

There are other cases in which only a part of a unit cell of one structure can, in combination with a unit cell of another one and by parallel intergrowth, originate another structure. Such is the case of $Ca_2LaFe_3O_8$, whose structure can be described (*7, 8*) as built up from a unit cell of perovskite and half a unit cell of brownmillerite according to

$$ABO_3 + \tfrac{1}{2}A_4B_4O_{10} \rightarrow A_3B_3O_8. \quad (1)$$

Although this phase appears, in the first instance, as just another example of one-dimensional intergrowth, the redox chemistry of $Ca_2LaFe_3O_8$ (*9, 10*) originates solid phases in which microdomains having this intergrowth structure are themselves intergrown in the three dimensions to build up the crystals (3D-μD). As such a microdomain texture appears to be an essential characteristic of the chemistry of these perovskite-based ferrites, it is important to know the role that different cations can play in microdomain formation. For this

0022-4596/86 $3.00

reason, we are performing a study of microdomain formation in perovskite-based ferrites in which iron is wholly or partially substituted by other transition metal cations. We report in this paper part of this work referring to the $Ca–Mn–Fe–O_2$ system. In a previous communication (*11*) we have shown that samples of this system with the $x = 0.4$ composition treated in air at 1400°C were made of crystals formed by six sets of microdomains disorderly intergrown in three dimensions. Of these six sets, three correspond to a $Ca_2Fe_2O_5$-type solid and the other three sets of a $CaMnO_3$-type solid. In an attempt to understand more deeply those microdomain textured solids we have performed a study of the oxidation and reduction of these samples. Previous evidence (*9, 10*) appears to suggest the existence of some relationship between the presence of microdomains and that of a tetravalent cation. All these samples are characterized by a small domain size, typically ~200 Å on a side, so that X-ray powder diffraction is less informative than electron microscopy and diffraction. These are the techniques that we have mainly used.

Experimental

All samples were prepared by means of the "ceramic procedure," namely, by heating the appropriate amounts of metal carbonates or oxides of Analar quality at the corresponding temperatures in air or in oxygen as described in the text in each case.

Chemical analysis. Total iron in the samples was determined by previously reducing it to the divalent state with a $SnCl_2$ solution in hydrochloric acid. The resulting Fe^{2+} was titrated with a $K_2Cr_2O_7$ solution in the presence of phosphoric acid.

The total manganese content of the samples was obtained after dissolving them in a mixture of nitric and phosphoric acids. Oxidation to permanganate by means of KIO_4 in the presence of phosphoric acid allowed the manganese content to be determined by spectrophotometry.

The amount of Mn^{4+} was obtained by dissolving the sample in hydrochloric acid and adding potassium iodide solution in the presence of acetylacetone. The iodine liberated was determined by titration with a $Na_2S_2O_3$ solution in the presence of starch.

Total amounts of manganese and iron were also obtained by atomic absorption spectrometry.

Products have been characterized by X-ray powder diffraction using silicon as internal standard.

Electron diffraction and microscopy have been performed on a Siemens Elmiskop 102 electron microscope fitted with a double tilting goniometer stage.

Results and Discussion

Figure 1 shows the X-ray diffraction patterns of the most representative samples. Figure 1a gives the pattern corresponding to the starting solid, i.e., $CaFe^{III}_{0.4}Mn^{III}_{0.22}Mn^{IV}_{0.38}O_{2.69}$ heated in air at 1400°C for 60 hr and quenched in air to room temperature. This relatively simple pattern can be indexed in terms of a cubic cell with $a = 3.776(1)$ Å. In spite of this simplicity, electron micrographs and diffraction patterns indicate a more complicated situation.

Figure 2 shows an electron micrograph and the corresponding electron diffraction pattern of the same sample. As shown elsewhere (*11*) they can be interpreted in terms of six sets of microdomains [cf. Introduction and Ref. (*11*)].

Annealing of this sample in air at 1000°C results in a sample which gives the X-ray diffraction pattern shown in Fig. 1b. With two exceptions, to be discussed below, all the lines in this pattern can be indexed on the basis of a cell multiple of the perovskite cell and with parameters $a_c\sqrt{2} \times 3a_c \times a_c\sqrt{2}$. This kind of multiple cell can itself be explained in terms of a structure intermedi-

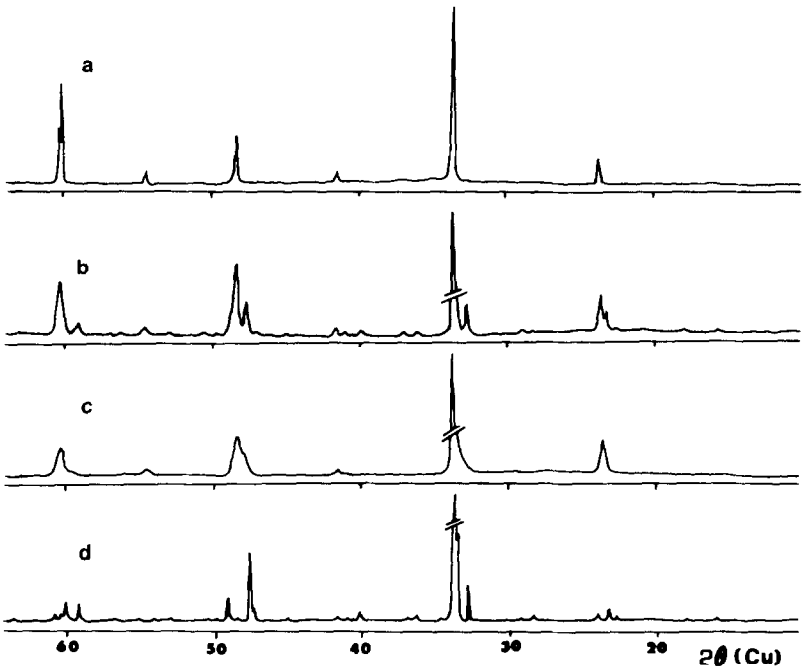

FIG. 1. X-Ray diffraction patterns ($\lambda CuK\alpha$ = 1.5418) of (a) $CaFe^{III}_{0.4}Mn^{III}_{0.22}Mn^{IV}_{0.38}O_{2.69}$ (1400°C, air); (b) (*a* + 1000°C, air, 72 hr); (c) (*a* + 1000°C, pO_2 = 1 atm, 28 hr), (d) (*c* + 1000°C, air, 24 hr).

ate between perovskite and brownmillerite. As shown by Grenier *et al.* (*7, 12*) the threefold superlattice corresponds to a sequence of polyhedra formed by two octahedra [FeO_6] and one tetrahedra [FeO_4], i.e., a unit cell of perovskite and half a unit cell of brownmillerite that follow each other along a perovskite subcell axis. With this sequence of polyhedra the resulting composition is $A_2B_2O_5$ + ABO_3, i.e., $A_3B_3O_8\langle\rangle ABO_{2.67}$. In our case, the analytical composition will be represented by $Ca Mn_{0.6}Fe_{0.4}O_{2.67}$. Recently, Nguyen *et al.* (*13*) have found this structure with a different composition $Ca_3Fe_{1.65}Mn_{1.35}O_{8.02}\langle\rangle CaFe_{0.55}Mn_{0.45}O_{2.67}$. This means that the range of existence of this threefold term extends at least between $0.40 \leq x \leq 0.55$. This annealing process eliminates the microdomains so that a very marked structural rearrangement of the oxygen and metal positions happens [cf. Ref. (*10*)] under these conditions. This complex process appears, however, to be reversible and heating at 1400°C in air reproduces the texturally complex starting solid, showing six sets of microdomains.

The two extra lines of the pattern in Fig. 1b that cannot be indexed on the $ABO_{8/3}$ cell within the space group *Pm2a* (as determined by Nguyen *et al.*) have *d* spacings of *d* = 3.765 Å and *d* = 1.684 Å, respectively, and could be indexed in the $CaMnO_3$ cell.

As all the three phases are superstructures of the perovskite cell, it is likely that some other lines belonging to $CaMnO_3$ are also present but overlap with those of the threefold superlattice. Likewise, some $Ca_2Fe_2O_5$ lines may be present but also overlap with those of both $CaMnO_3$ and $Ca_3Mn_{1.8}Fe_{1.2}O_8$. This simply means that part of the starting solid is still unreacted. In any event, the amount present must be very minute since the extra lines are weak and

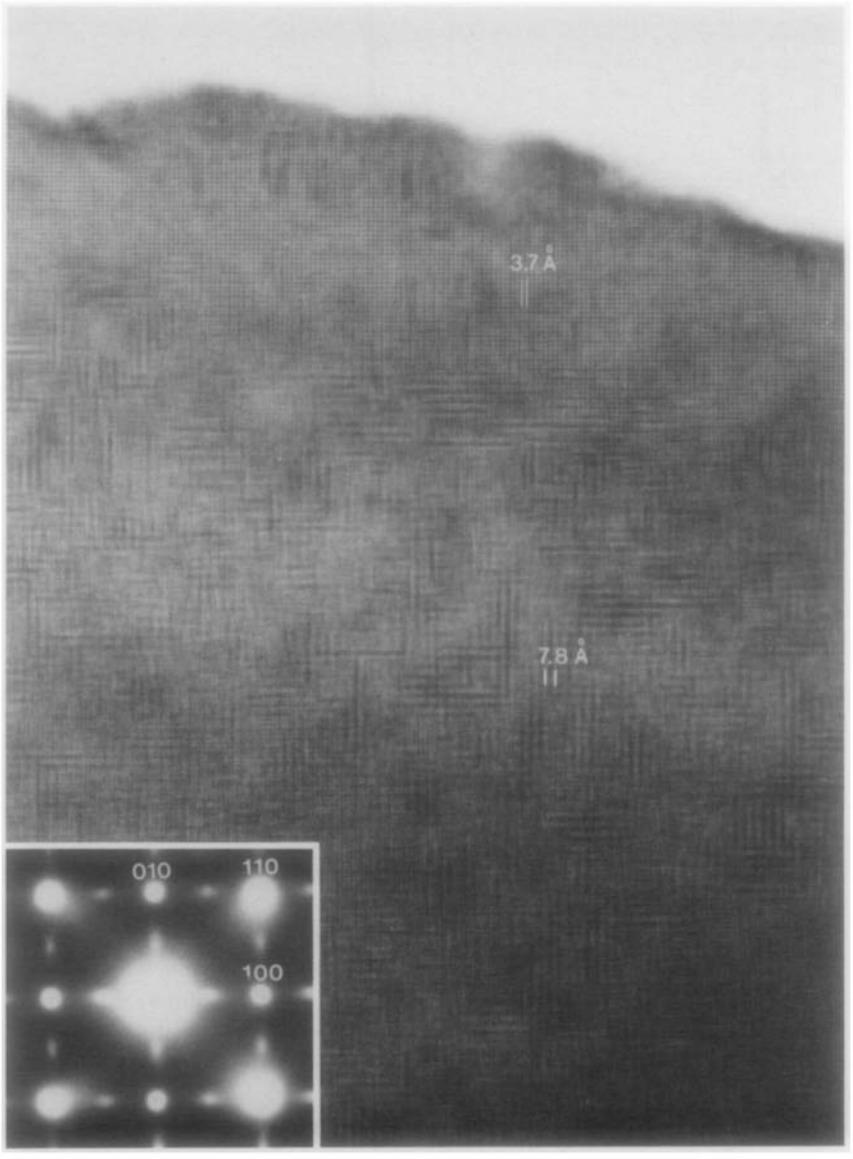

FIG. 2. Electron micrograph and diffraction pattern of the starting sample.

we did not see any of those crystals on the normal electron microscopic observations.

Reduction in Argon

Treating the starting sample in argon at 1000°C ($P_{O_2} \simeq 10^{-7}$ atm) a totally different situation occurs and two phases appear as suggested by X-ray diffraction. One of them is unmistakable brownmillerite-type $Ca_2Fe_2O_5$, which was also identified by electron diffraction.

As for the other one, it is more difficult to establish unambiguously its composition since the X-ray lines not indexed with the

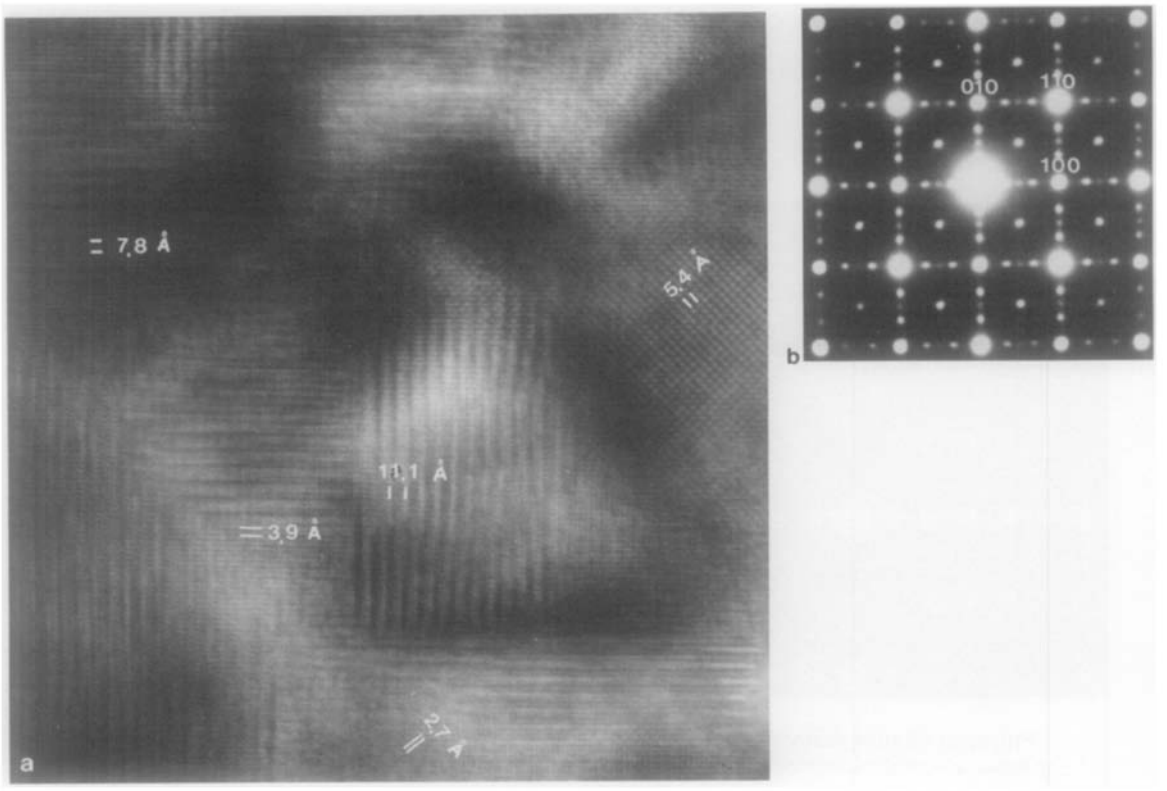

hkl	Phase	distance (Å)
010	$Ca_3(Mn_{1-x}Fe_x)_3O_8$	11.1
010	$CaMnO_3$	
020	$Ca_2Fe_2O_5$	7.6
100	$Ca_2Fe_2O_5$	
or	$CaMnO_3$	
001	$Ca_3(Mn_{1-x}Fe_x)_3O_8$	5.4
101	$Ca_3(Mn_{1-x}Fe_xO)_3O_8$	3.9
200	$Ca_2Fe_2O_5$	
or	$CaMnO_3$	
002	$Ca_3(Mn_{1-x}Fe_x)_3O_8$	2.7

FIG. 3. (a) Electron micrograph of the sample oxidized in pure oxygen. (b) Corresponding electron diffraction pattern.

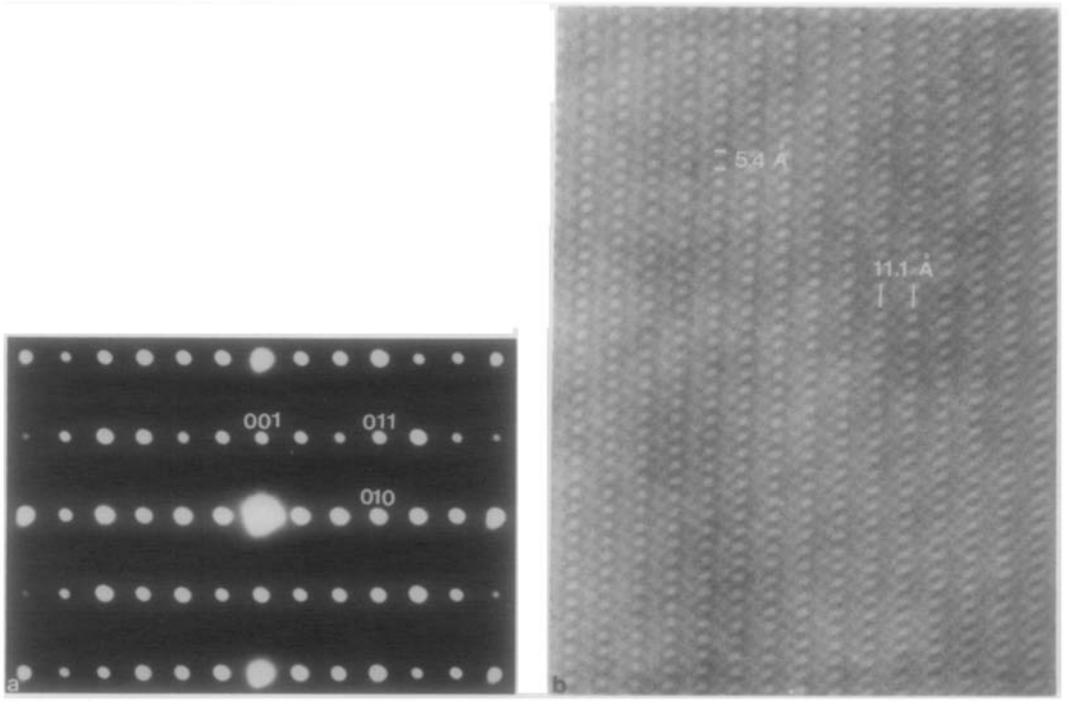

FIG. 4. (a) Electron diffraction pattern of the $Ca_3(Fe_xMn_{1-x})_3O_8$ along the [100] zone axis. (b) Corresponding electron micrograph.

$Ca_2Fe_2O_5$ cell can be indexed fully or partly with the cells corresponding to $CaMnO_{2.67}$, $CaMnO_{2.55}$ (*14*), and even $Ca_2Mn_2O_5$ as proposed by Poeppelmeier *et al.* (*15*).

Highly Oxidating Conditions

The final process to which our sample was submitted was an oxidation process in pure oxygen at high temperature (1000°C) during 28 hr. As in the original sample, the X-ray diffraction pattern (Fig. 1c) was, apart from some broadening of the lines, deceptively simple and could be indexed on the basis of a cubic perovskite cell with parameter $a = 3.760(1)$ Å.

Nevertheless, by electron microscopy and diffraction a novel situation appeared: microdomains were not only preserved but the number of microdomain sets present in the crystals increased to nine, instead of six in the original sample. Figure 3a shows an electron micrograph of this sample in which the presence of microdomains is plain. Several sets of fringes with different spacings are observed. According to previous work they can be attributed to the *d* spacings detailed in Fig. 3a. The corresponding electron diffraction pattern (Fig. 3b) shows all the maxima appearing in Fig. 2 plus another three sets of maxima. These new three sets correspond, in fact, to a microdomain textured solid whose threefold superstructure (analogous to that shown in Fig. 4) allows one to interpret it as belonging to a $Ca_3(Mn_{1-x}Fe_x)_3O_8$-type phase intergrowth with $Ca_2Fe_2O_5$ and $CaMnO_3$ in the three dimensions. Several other reciprocal lattice sections, not shown, did indeed confirm this interpretation and as a result we have to describe the oxidation process of our sample in two ways:

TABLE I
UNIT CELL PARAMETERS

Phase	Unit cell parameter (Å)	Cubic perovskite parameter (Å)
$CaMnO_3$	$a = 5.279(1)$ $b = 7.448(1)$ $c = 5.264(1)$	3.726
$CaFe^{III}_{0.4}Mn^{III}_{0.22}Mn^{IV}_{0.38}O_{2.69}$	$a = 3.776(1)$	3.776
$CaFe^{III}_{0.05}Fe^{IV}_{0.35}Mn^{III}_{0.39}Mn^{IV}_{0.21}O_{2.78}$	$a = 3.760(1)$	3.760
$CaFe^{III}_{0.4}Mn^{III}_{0.25}Mn^{IV}_{0.35}O_{2.675}$	$a = 5.343(1)$ $b = 11.17(1)$ $c = 5.457(2)$	3.786
$Ca_2Fe_2O_5$	$a = 5.4253(5)$ $b = 14.7687(17)$ $c = 5.5980(5)$	3.829

(1) Structurally

$$\begin{pmatrix}\text{3D-}\mu\text{D } a\text{Ca}_2\text{Fe}_2\text{O}_5\\ \text{3D-}\mu\text{D } b\text{CaMnO}_3\end{pmatrix} + \text{O}_2 \rightarrow \begin{pmatrix}\text{3D-}\mu\text{D } a'\text{Ca}_2\text{Fe}_2\text{O}_5\\ \text{3D-}\mu\text{D } b'\text{CaMnO}_3\end{pmatrix} + \text{3D-}\mu\text{D Ca}_3(\text{Mn}_{1-x}\text{Fe}_x)_3\text{O}_8 \quad (2)$$

recalling the textural complexity of the samples.

(2) In chemical analytical terms, the reaction can be expressed in accordance with the following compositions:

$$CaFe^{III}_{0.4}Mn^{III}_{0.22}Mn^{IV}_{0.38}O_{2.69} + \frac{0.09}{2}O_2 \rightarrow CaFe^{III}_{0.05}Fe^{IV}_{0.35}Mn^{III}_{0.39}Mn^{IV}_{0.21}O_{2.78} \quad (3)$$

which reflect the nonstoichiometric nature of the system.

When this highly oxidized sample was annealed in air at 1000°C for 3 days the product was pure $Ca(Mn_{1-x}Fe_x)O_{8/3}$ as shown by X-ray diffraction (Fig. 1d), where no extra lines appear. The whole pattern can be indexed in a unit cell with the parameters shown in Table I. Electron microscopy and diffraction confirmed such an interpretation. The diffraction pattern (Fig. 4a) has been indexed in the $a_c\sqrt{2} \times 3a_c \times a_c\sqrt{2}$ cell, superstructure of the perovskite cell. In the corresponding micrograph crossed fringes with separation 5.5 and 11.1 Å indicate the unit cell projected along a. A higher resolution study to analyze in detail this type of image is in progress and will be reported in due course. Chemical analysis indicated the absence of Fe(IV), the composition obtained being $Ca_3Fe^{III}_{1.2}Mn^{III}_{0.75}Mn^{IV}_{1.05}O_{8.025}$.

Figure 5 shows schematically the ensemble of all the processes studied in the present work.

Although these compositions do not reveal the elaborated, textural nature of the reaction, Eq. (3) shows that a very subtile redox process takes place within the crystal. In this process some Fe(III) goes to Fe(IV) while, simultaneously, some Mn(IV) goes to Mn(III). It also appears that the presence of Fe(IV) is instrumental in allowing the formation of three-dimensional microdomains of the $ABO_{8/3}$ phase, confirming previous evidence (*9, 10*), since, under milder oxidation conditions, no such microdomains appear and no Fe(IV) can be observed.

Moreover, it could be speculated that under sufficiently strong oxidizing conditions all the solid will convert to μD of the $ABO_{8/3}$ phase, such as happens in the case of $Ca_2LaFe_3O_8$ where this occurs even in air at 1400°C. Indeed, under even stronger oxidizing conditions, i.e., if all the B cations were in the IV oxidation state, a perovskite, ABO_3, should be obtained.

As indicated above, Nguyen *et al.* have studied a solid with general formula $ABO_{8/3}$ (*13*), where there are three different B cations distributed in three types of sites: Fe(III), Mn(III), and Mn(IV) within octahedra, tetrahedra, and square pyramids. The determination of the cation positions has, in that case, been estimated from the X-ray structure determination coupled with the Mössbauer analysis. These authors observed that, in the case of $Ca_3Mn_{1.35}Fe_{1.65}$

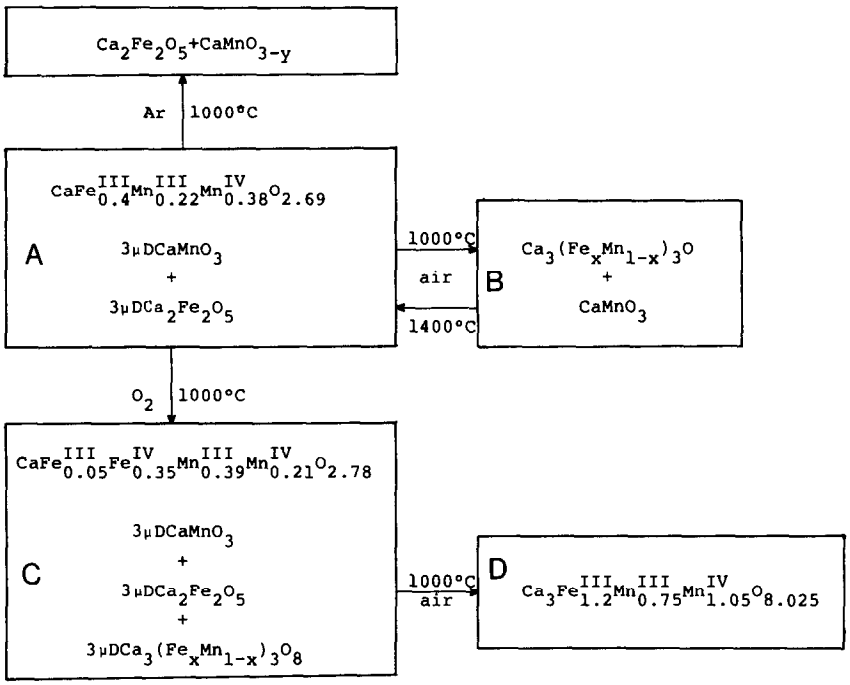

FIG. 5. Schematic representation of the studied processes.

$O_{8.02}$, the occupation factor of the O_3 positions, corresponding to an octahedron, was 70% instead of 100%, while that of O'_5, which is next to a tetrahedron and should be unoccupied in the normal $ABO_{8/3}$ structure, was occupied at 30%.

In our case, however, we have four B cations, Fe(III), Fe(IV), Mn(III), and Mn(IV), and, even neglecting the domain walls, in the μD-textured solid they have to be distributed in three types of octahedral sites—corresponding to $CaMnO_3$, $Ca_2Fe_2O_5$, and $Ca_3(Mn_{1-x}Fe_xO_8)$—plus two types of tetrahedral sites and presumably some square pyramids; also the calcium ions are located in different types of sites. In this case, it is certainly not obvious as to how to establish the cation distribution among all those sites. However, it is clear that the calcium ions are indistinguishable so that their final positions are always equivalent. On the other hand, there is no evidence of B cations ordering in any of those perovskite-based substituted ferrites so that, in principle, with just electrons and oxygen diffusion the whole process of domain multiplication or elimination can be accounted for. For those reasons these materials are worth testing as oxido-reduction catalysts (*16*). The above reasoning certainly does not mean that the cations are fixed when the sample is at, for example, ~1400°C in air or at 1100°C under argon. Simple calculations based on random-walk theory (*17*) indicate that in one day, an iron ion in the closely related $LaFeO_3$, with a diffusion coefficient of 5×10^{-12} cm²/sec (*18*), will have an average displacement of ~2 cm.

If we now consider the pseudocubic cell parameter of all these phases, an almost linear correlation is observed between this average dimension and the amount of trivalent cation present on the solid (Fig. 6). This is, indeed, what one would expect in view of the ionic sizes of tri- and tetravalent

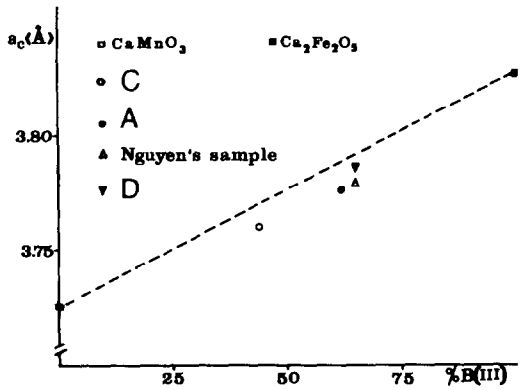

FIG. 6. Evolution of the pseudocubic cell parameter of the $CaFe_xMn_{1-x}O_{3-y}$ samples with the percentage of trivalent cation.

cations in octahedral, tetrahedral, and square pyramidal coordinations (*19*). An interesting point is that all our samples as well as Nguyen's sample fit this correlation independently of being normal or microdomain textured. In general, then, size factors made a strong influence on the unit cell dimensions of this series.

In a very similar system based in the brownmillerite structure, and with general formula $Ca_2Mn_xFe_{2-x}O_{5+\delta}$, Akiyama (*20, 21*) has found a so-called ordered phase. His samples were prepared under very strong oxidizing conditions and their oxygen content is, in some cases, similar to that expected for the $ABO_{8/3}$ formula or to the more oxidized ones, up to $ABO_{2.735}$. Although to index its diffraction patterns, Akiyama uses a doubled brownmillerite cell, it is not clear what ordering pattern such a cell represents. In any event, notwithstanding that the Fe/Mn ratio of the Akiyama sample is different from ours, being Fe richer, one would expect that, if the superstructure is due to an oxygen ordering along an octahedron–octahedron–tetrahedron sequence, a normal $ABO_{8/3}$ cell, or a polytype of it, should be observed when the composition is $ABO_{2.69}$, and some form of microdomains are likely be present in his $ABO_{2.73}$ sample. Certainly an electron microscopy and diffraction study of those samples will be needed to test such a possibility.

References

1. S. ANDERSSON, *Angew. Chem.* **22,** 69 (1983).
2. C. N. R. RAO AND J. M. THOMAS, *Acc. Chem. Res.*, in press.
3. L. KIHLBORG, *Chem. Scr.* **14,** 187 (1978–1979).
4. L. A. BURSILL AND B. G. HYDE, *Philos. Mag.* **20,** 347 (1969).
5. S. ANDERSSON AND L. STENBERG, *Z. Kristallogr.* **158,** 133 (1982).
6. A. SIMON, *Z. Anorg. Allg. Chem.* **422,** 208 (1976).
7. J. C. GRENIER, J. DARRIET, M. POUCHARD, AND P. HAGENMULLER, *Mater. Res. Bull.* **11,** 1219 (1976).
8. J. M. GONZÁLEZ-CALBET, M. VALLET-REGÍ, M. A. ALARIO-FRANCO, AND J. C. GRENIER, *Mater. Res. Bull.* **18,** 285 (1983).
9. M. A. ALARIO-FRANCO, M. J. R. HENCHE, M. VALLET REGÍ, J. M. GONZÁLEZ-CALBET, J. C. GRENIER, A. WATTIAUX, AND P. HAGENMULLER, *J. Solid State Chem.* **46,** 23 (1983).
10. J. M. GONZÁLEZ-CALBET, M. VALLET-REGÍ, AND M. A. ALARIO-FRANCO, *J. Solid State Chem.* **60,** 320 (1985).
11. M. VALLET-REGÍ, J. M. GONZÁLEZ-CALBET, J. VERDE, AND M. A. ALARIO-FRANCO, *J. Solid State Chem.* **57,** 197 (1985).
12. J. C. GRENIER, G. SCHIFFMACHER, P. CARO, M. POUCHARD, AND P. HAGENMULLER, *J. Solid State Chem.* **20,** 365 (1977).
13. N. NGUYEN, Y. CALAGE, F. VARRET, G. FEVEY, V. CAISGNAERT, M. HERVIEU, AND B. RAVEAU, *J. Solid State Chem.* **53,** 398 (1984).
14. A. RELLER, J. M. THOMAS, D. A. JEFFERSON, AND M. K. UPPAL, *Proc. R. Soc. London, Ser. A* **394,** 223 (1984).
15. K. R. POEPPELMEIER, M. E. LEONOWICZ, J. C. SCANLON, J. M. LONGO, AND W. B. YELON, *J. Solid State Chem.* **45,** 71 (1982).
16. R. J. VOORHOEVE, *Adv. Mater. Catal.* **129,** 180 (1977).
17. P. G. SHEWMON, "Diffusion in Solids," Chap. 2, McGraw–Hill, London (1963).
18. T. ISHIGAKI, S. YAMAUCHI, J. MIZUSAKI, K. FUEKI, H. NAITO, AND T. ADACHI, *J. Solid State Chem.* **55,** 50 (1984).
19. R. D. SHANNON AND C. T. PREWITT, *Acta Crystallogr. Sect. B* **25,** 925 (1969).
20. T. AKIYAMA, *Mater. Res. Bull.* **16,** 469 (1981).
21. T. AKIYAMA, *Mater. Res. Bull.* **16,** 1077 (1981).